Roles of the westward propagating waves and the QBO in limiting MJO propagation

Kai Huang[1] and Kathleen Pegion[2]

[1]George Mason University Fairfax
[2]George Mason University

November 21, 2022

Abstract

A recent study categorized the Madden-Julian Oscillation (MJO) during the boreal winter season into four types including stand, jump, slow eastward propagating, and fast eastward propagating MJO. This study focuses on the stand and jump MJO events. Based on whether their convection penetrates the Maritime Continent (MC), stand and jump MJO are combined as non-penetrating (NP) MJO, while the rest two types are combined as eastward-penetrating (EP) MJO. Results reveal the relative roles of the westward-propagating wave (WPW), as well as the QBO and ENSO, in limiting MJO propagation. Lack of the pre-moistening over the southern sea surface of MC is responsible for NP MJO's failure to penetrate MC. The active convection of WPW hinders the NP MJO descending branch over the Pacific and therfore leads to the insufficient meridional advective moistening over the southern sea surface of the MC. The overall drying over the MC for jump MJO also comes from the intraseasonal dry amonalies induced by WPW over the western Pacific, which are then advected to MC by the superposed seasonal mean northern easterlies. The independent convection over the Pacific for jump MJO is influenced by a combined effect of the QBO and ENSO. Under the influence of the preferred QBO westerly (QBOW) phase, the tropopause instability of NP MJO is decoupled with its convection. The decoupled tropopause instability propagates eastward into the Pacific, and amplifies the local WPW convection there for jump MJO. For stand MJO, however, the La Nina-like seasonal mean cool sea surface temperature (SST) anmalies confine WPW within the western Pacific. Therefore, the decoupled tropopause instability of stand MJO is out phase of WPW over the central Pacific, and fails to induce an independent convection as a result. The similar diagnosis is further applied to the CESM2 and E3SM CMIP6 historical simulations to investigate the MJO diversity and propagation in climate models. Four MJO types as in the observation are successfully categorized in these two models. The accompanied westward propagating waves over the central-western Pacific for NP MJO events are also evident. However, models suffer from some biases in MJO propagation such as too many NP MJO events than the observation.

Abstract ID: 917295

Roles of the westward propagating waves and the QBO in limiting MJO propagation

Kai Huang*, Kathleen V. Pegion
Department of Atmospheric, Oceanic, and Earth Sciences
George Mason University

I. Four types of MJO

1. Apply the k-means cluster analysis by OLR Hovmöller diagrams of MJO cases.
2. Examine the silhouette score for each cluster member.

+Details can be found in Wang et al., 2019

➢ Data
- Era-Interim Reanalysis
- NCEP/NOAA-interpolated OLR
- Extended Reconstructed Sea Surface Temperature version 5 (ERSSTv5) dataset

➢ Method
- Composite analysis
  - student-t significance test
- Moisture budget analysis

Non-Penetrating (NP) and Eastward-Penetrating (EP) MJO

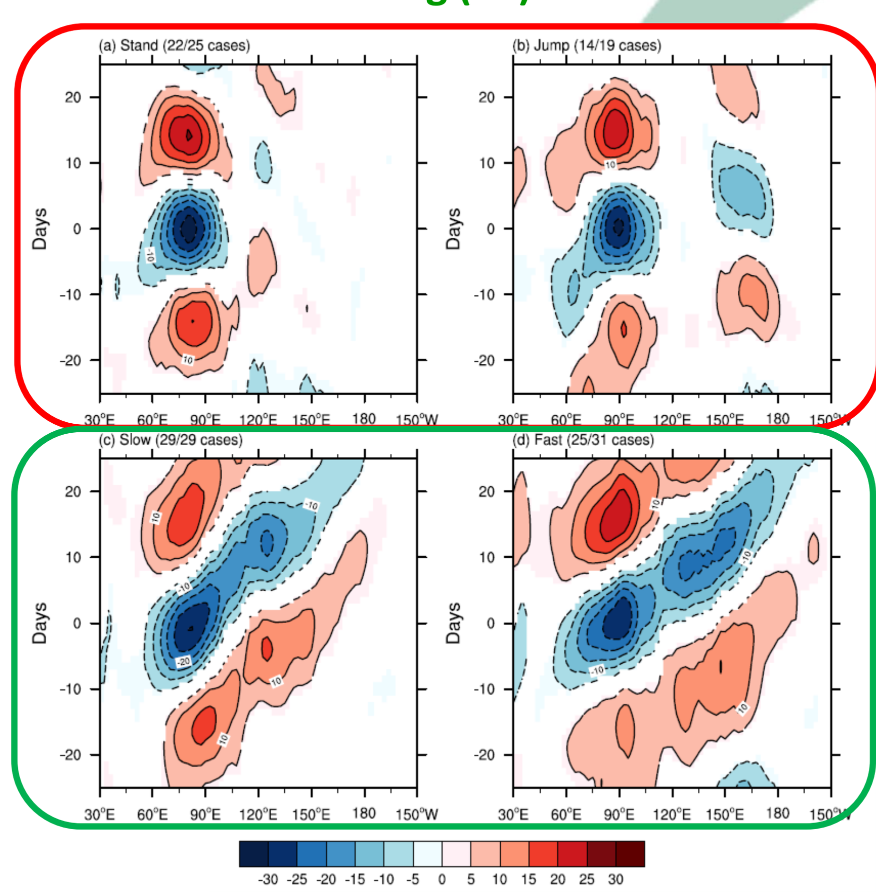

Fig. 1 Composited OLR Hovmöller diagrams (10S-10N) for four types of 104 MJO cases identified in 1979-2013. Stand and Jump MJO cases are viewed as non-penetrating (NP) MJO while slow and fast MJO cases are seen as eastward-penetrating (EP) MJO.

II. QBO and ENSO phase preferences among MJO types

➢ **NP MJO:**
- An apparent preference of QBOW phase.
  - Stand MJO: a preference of La Nina condition.

➢ **EP MJO:**
- No preference of QBO phase.
  - Fast MJO: a preference of El Nino condition.

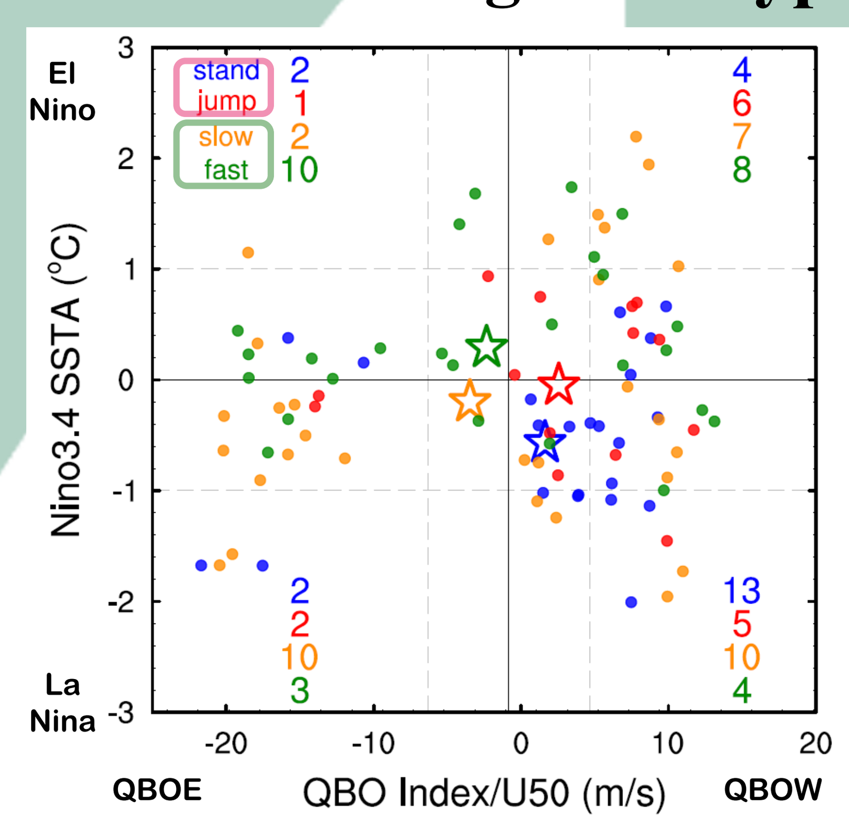

Fig. 2 Phase diagram of QBO and ENSO for MJO cases. X axis refers to the QBO index defined as global mean of equatorial (5S-5N) monthly zonal wind. Y axis refers to the ENSO index using monthly Nino3.4 index.

***Contact: Kai Huang, khuang8@gmu.edu**

+Wang B, Chen G, Liu F. Diversity of the Madden-Julian oscillation[J]. Science Advances, 2019, 5(7): eaax0220.

III. Disrupted pre-moistening over MC due to westward-propagating waves (WPW)

➢ NP MJO

i.
Active convection of WPW hinders the descending branch of MJO circulation.

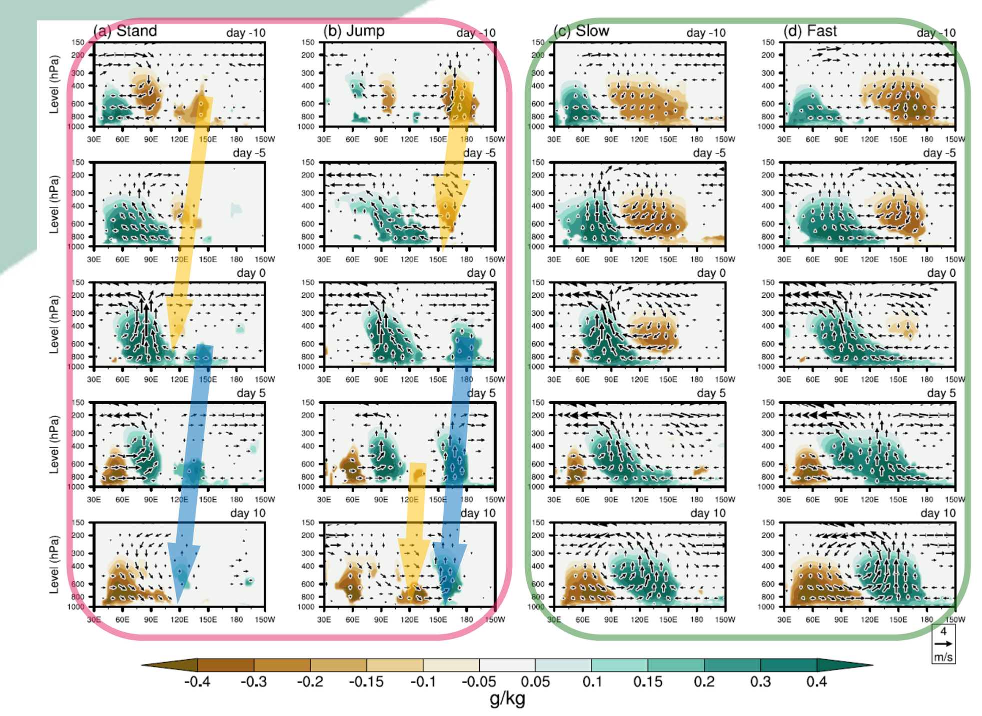

Fig. 3 Vertical sections of equatorial intraseasonal wind (vectors) and specific humidity (shadings) anomalies for four MJO types.

ii.
Weakened/missing poleward wind anomalies over the southern sea surface of MC.

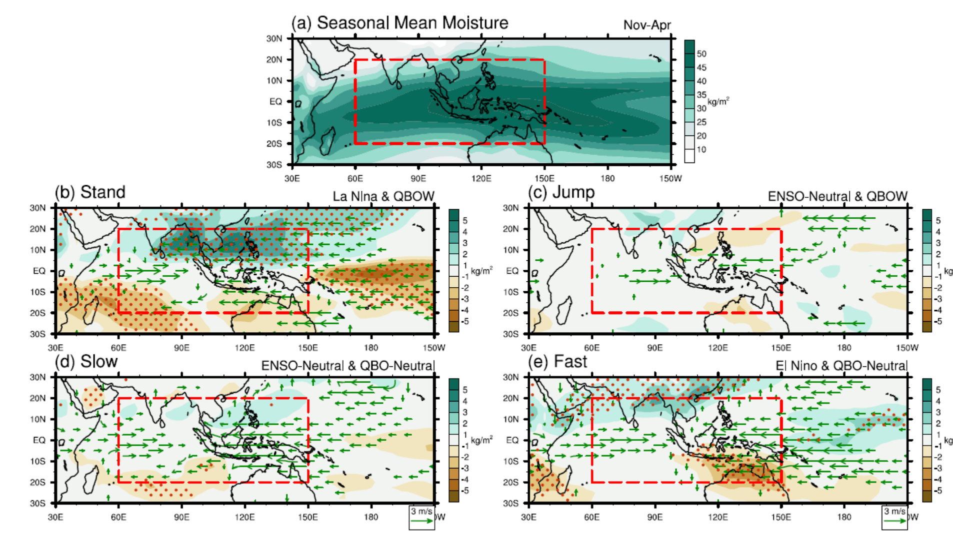

Fig. 4 Composited maps of (a) seasonal-mean integrated (surface to 100hPa) specific humidity climatology, (b)-(d) intraseasonal wind anomalies (vectors) and deviations of the integrated specific humidity from its climatology in (a) for four MJO types.

iii.
Insufficient meridional moisture advection leads to in sufficient pre-moistening over the southern sea surface of MC.

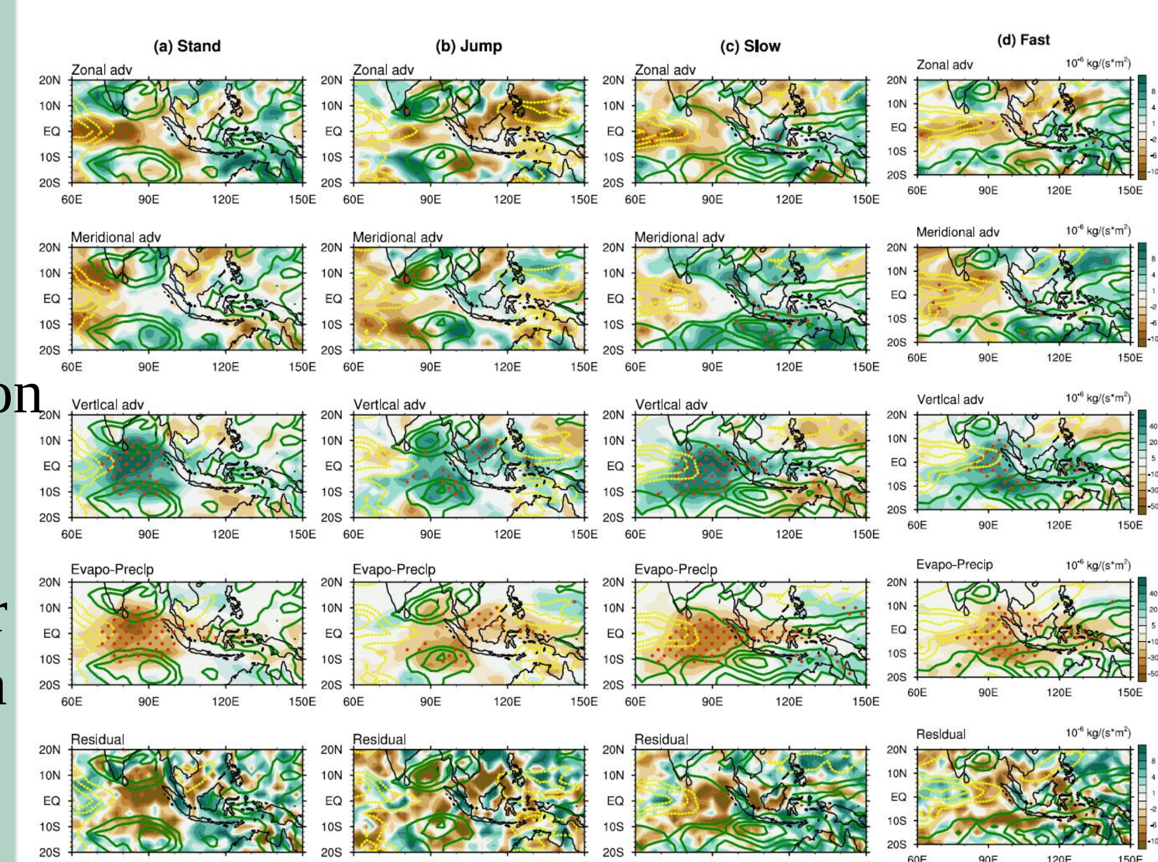

Fig. 5 Composited maps of intraseasonal moisture tendencies (lines) and right-hand-side terms of moisture budget analysis (shadings) for four MJO types.

IV. Decoupled tropopause instability due to preferred QBOW phase

➢ **NP MJO**
- Dissipated heating structure.
- Decoupled, propagating tropopause instability.

➢ **EP MJO**
- Well-organized heating structure.
- Coupled tropopause instability.

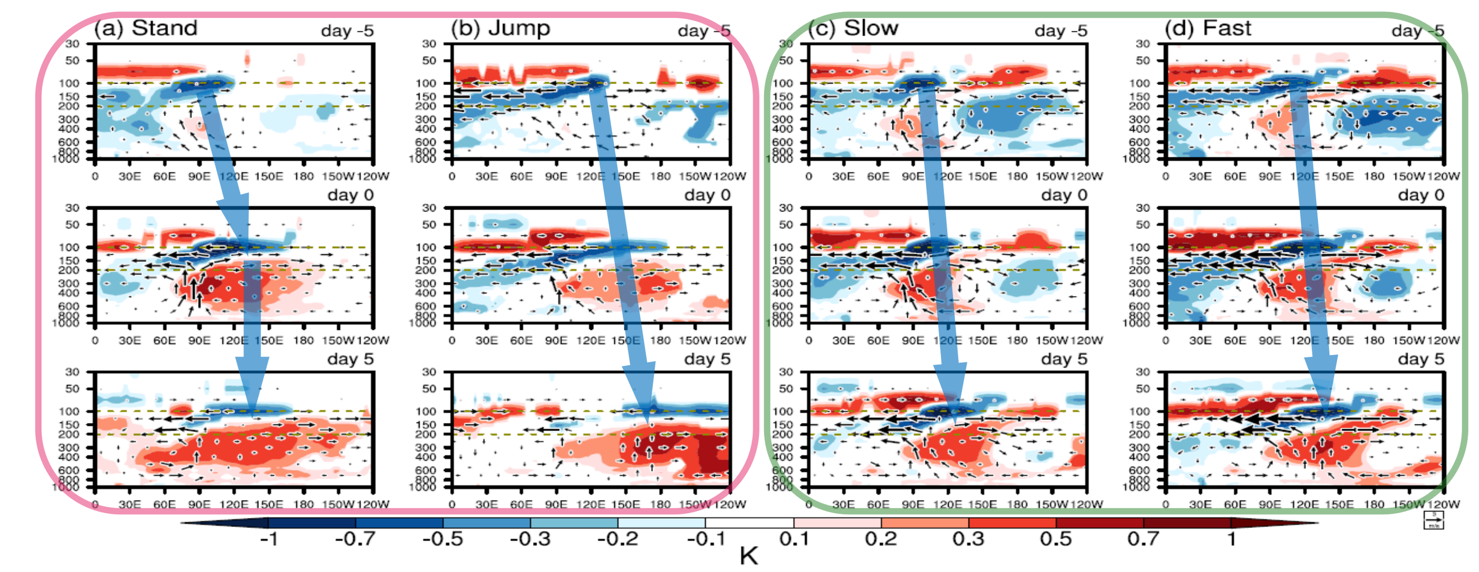

Fig. 6 Vertical sections of equatorial intraseasonal wind (vectors) and temperature (shadings) anomalies for four MJO types.

➢ **NP MJO**

Fails to penetrate MC due to missing pre-moistening caused by WPWs

- **Jump MJO (QBOW)**

Decoupled tropopause instability enhances WPWs over central Pacific and leads to the independent convection as in Fig. 1b.

- **Stand MJO (QBOW + La Nina)**

Decoupled tropopause instability, but La Nina-like cool SST confines WPW over western Pacific.

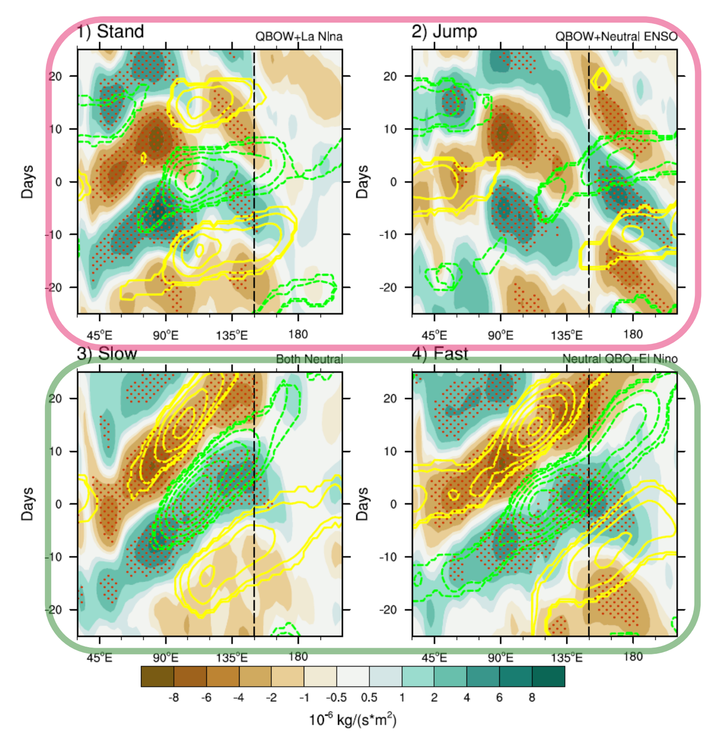

Fig. 7 Hovmöller diagrams (10S-10N) of intraseasonal tropopause instability (T100-T200, lines) and moisture tendency (shadings) for four MJO types.

V. Caveats and future work

❑ Limited sample size especially for jump MJO cases.

❑ Correlation does not guarantee causality.

✓ Diagnostics and sensitivity experiments using climate models.

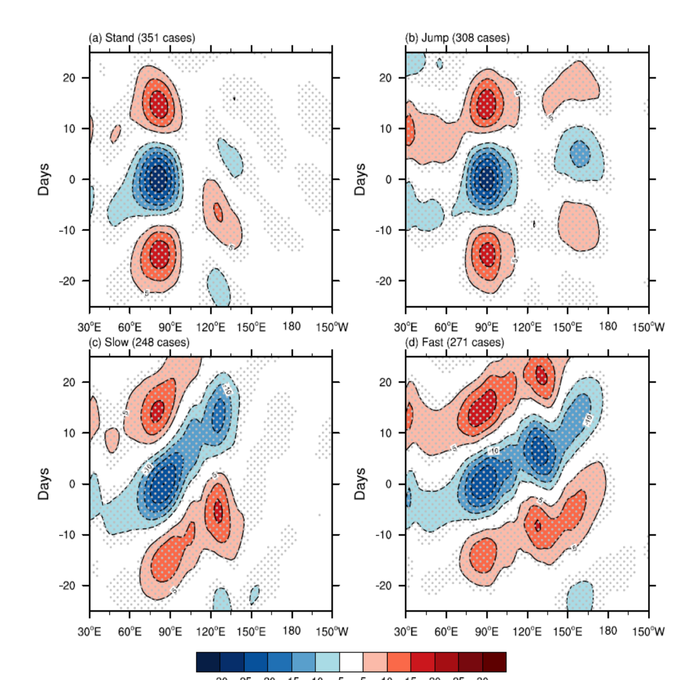

Fig. 8 OLR Hovmöller diagrams (10S-10N) of for four types of 1,178 MJO cases in CESM2 historical ensemble simulations for CMIP6.